

# Comparison of Support Vector and Non-Linear Regression Models for Estimating Large-Scale Vehicular Emissions, Incorporating Network-Wide Fundamental Diagram for Heterogeneous Vehicles

Ramin Saedi<sup>1</sup>, Rajat Verma<sup>1</sup>, Ali Zockaie<sup>1</sup>, Mehrnaz Ghamami<sup>1</sup>, and Timothy J. Gates<sup>1</sup>

## Abstract

Estimation of vehicular emissions at network level is a prominent issue in transportation planning and management of urban areas. For large networks, macroscopic emission models are preferred because of their simplicity. However, these models do not consider traffic flow dynamics that significantly affect emissions production. This study proposes a network-level emission modeling framework based on the network-wide fundamental diagram (NFD), via integrating the NFD properties with an existing microscopic emission model. The NFD and microscopic emission models are estimated using microscopic and mesoscopic traffic simulation tools at different scales for various traffic compositions. The major contribution is to consider heterogeneous vehicle types with different emission generation rates in a network-level model. This framework is applied to the large-scale network of Chicago as well as its central business district. Non-linear and support vector regression models are developed using simulated trajectory data of 13 simulated scenarios. The results show a satisfactory calibration and successful validation with acceptable deviations from the underlying microscopic emissions model regardless of the simulation tool that is used to calibrate the network-level emissions model. The microscopic traffic simulation is appropriate for smaller networks, while mesoscopic traffic simulation is a proper means to calibrate models for larger networks. The proposed model is also used to demonstrate the relationship between macroscopic emissions and flow characteristics in the form of a network emissions diagram. The results of this study provide a tool for planners to analyze vehicular emissions in real time and find optimal policies to control the level of emissions in large cities.

The environmental impacts of vehicular traffic in urban transportation networks have been extensively studied. It is widely accepted that pollutants emitted from on-road vehicles constitute a majority of air pollutants in urban environments (1) and have grave consequences for human health and climate change (2, 3). In 2012, poor air quality because of vehicular emissions was estimated to cause about 3.7 million premature deaths worldwide, which is expected to rise considerably in the next few decades (4). Thus, a systematic manner of investigation and policy making is required to manage the generation of emissions, specifically in large cities. This calls for a tool that can provide quick and accurate estimates of emissions at the network level under each proposed policy or strategy. Since accurate measurements in real networks are highly

difficult, empirical estimation and modeling of vehicular emissions has become an important activity in the disciplines of urban planning and transportation management.

The existing body of work on estimation of vehicular emissions can be broadly categorized into three types of techniques: microscopic, macroscopic, and mesoscopic modeling. Microscopic modeling is common in emission estimation at both vehicular and network levels (5, 6). These models invariably rely on vehicular motion state

<sup>1</sup>Department of Civil and Environmental Engineering, Michigan State University, East Lansing, MI

**Corresponding Author:**

Ali Zockaie, zockaiea@egr.msu.edu

characteristics, such as speed and acceleration, rather than vehicle-specific characteristics like engine specification or driver behavior (7, 8). While average speed models neglect the role of speed fluctuations (8, 9), instantaneous speed models are more robust in capturing traffic flow dynamics. They use speed and acceleration profiles of individual vehicles to calculate vehicle measures such as vehicle specific power, which in turn are used to build emission estimates (10–12). Normally, these detailed profiles are created by using an equivalent microscopic traffic assignment model and used simultaneously to generate the values of emission (11). CMEM and MOVES Lite are examples of software packages that work on this principle. Alternatively, detailed vehicle trajectories are generated using traffic micro-simulators like PTV Vissim, Paramics, and Aimsun (13, 14), which are then used to estimate emission on a second-by-second basis (15). This process is resource intensive, however, and is therefore not preferred for large systems such as urban road networks.

Macroscopic emission models, on the other hand, are used on relatively large scales such as the zone or network level. They typically use aggregate properties like traffic flow and density to estimate network-wide emissions without needing to evaluate the variation of traffic and emission variables at the individual level (16). Popular packages like MOBILE (17), EMFAC (18), and COPERT (19) make use of macroscopic emission models. While macroscopic models can be used to approximate emissions on large scales, they systematically ignore important actions and interactions such as vehicle acceleration and braking that form an integral part of the more accurate microscopic models.

Mesoscopic models lie between microscopic and macroscopic models in both scope and utility. They typically operate on presumably homogeneous platoons within the network based on traffic characteristics and therefore present a somewhat reasonable approximation of microscopic effects of traffic dynamics without significant addition in resource complexity. The VT-Meso modeling framework proposed by Zegeye et al. (12), for example, requires using a micro-emission model, VT-Micro (20), on such homogeneous platoons, which are computed based on the unrealistic assumption of absolute homogeneity of traffic composition. Despite the apparent advantages of mesoscopic models, the application of such hybrid approaches in emission estimation is currently limited to basic isolated networks, such as freeways (12), signalized intersections (21), and simple theoretical networks (22). The lack of effective tools, therefore, necessitates the development of a quick and effective technique for large-scale emission approximation, such as in urban environments that consist of different types of roadways and intersections.

This study uses an approach similar to previous studies (12, 22) to develop an emission estimation framework for large urban networks. In doing so, it also seeks to demonstrate that while micro-emission tools provide the necessary insight into the underlying mechanisms of emission models, they are not easily scalable and fail at high levels of network complexity. Therefore, macroscopic and mesoscopic tools must be exploited to facilitate such large-scale estimation. A simplified method of this approach is shown by Shabihkhani and Gonzales in an ideal ring model (23) but has not seen application on large real urban road networks. Moreover, the model proposed by Shabihkhani and Gonzales (23) is not sensitive to different vehicle types (in relation to emission efficiency).

This paper presents three main contributions. First, a general framework to produce a network-wide emission estimation model that can be easily and reliably used by urban transportation planners and agencies is proposed. The presented framework is flexible with respect to modeling parameters such as the choice of the base micro-emission model and traffic which may be at the planners' discretion. It may find applications in real-time traffic management as well as urban planning in cases such as the incorporation of alternative fuel vehicles. Second, it addresses some key issues associated with current macro-emission estimation techniques. (a) It demonstrates the effectiveness of mesoscopic traffic simulation in estimating emissions at a large scale with significantly low resource consumption compared with microscopic models. (b) It offers a way to include different vehicle classes without the loss of generality for generating network-wide fundamental diagrams by considering their fuel type. (c) It allows for the inclusion of an array of road network elements in simulation and emission estimation, including freeways, arterial roads, signalized intersections, and interchanges. Third, the relationship between network-wide fundamental diagram and macro-emission is also discussed in the form of a three-dimensional diagram here called the network emission diagram (NED). This presents a qualitative interpretation of the emission behavior of the network at different stages of its loading cycle. This is similar to other diagram-based concepts developed in the literature, such as the macroscopic surrogate safety diagram (24).

The proposed framework in this study can stipulate a new generation of traffic control strategies to mitigate the vehicular emissions in a congested part of the network by gating the travel of excessively inefficient vehicles in relation to emission to that area. This study paves the way to achieve this objective by proposing a framework to monitor emission generation dynamics in real time. Moreover, the formulated framework can be extended to predict network-level impacts of deployment

of new generations of vehicles such as electric and hydrogen powered vehicles.

The rest of the paper is organized as follows. In the 'Background and Modeling Tools' section the materials utilized in the modeling framework are discussed. The 'Modeling' section describes the specifications of the proposed framework. These specifications are tested in the 'Numerical Experiment' section. The results obtained are used to generate an NED, whose properties are discussed in the 'Network Emission Diagram' section. Concluding remarks are presented in the 'Conclusions' section.

## Background and Modeling Tools

### Network Fundamental Diagram

Network fundamental diagram (NFD), also known as macroscopic fundamental diagram (MFD), is a network-level concept of traffic flow theory. The concept of NFD is based on the fundamental diagram of individual road network links as aggregated on a macroscopic level (25). It shows the relationship between the network production and accumulation on road networks. NFD can also be expressed as relations between network-wide averages of link flow and density (26). Researchers have proposed different methods to estimate NFD, such as the use of space-time three-dimensional vehicle trajectories (27) and formulating a resource allocation problem to account for limited resources in real networks for data collection, traffic heterogeneity, and asymmetry in origin-destination demand (28, 29).

NFD is an important indicator of the network-wide traffic state and is used to compare the performance, stability, travel time reliability, and congestion characteristics of urban networks (25, 30–32). The NFD can be estimated using a traffic simulator, sampled observations of loop detectors, and vehicle trajectories, or by using an analytical approach (28). While existing research advocates the use of NFD in improving transportation management of an urban network, there is no sufficient literature on its potential in estimating air pollution over the network. This paper is an attempt to constructively bridge this gap.

In this study, the relationship between network-wide weighted average traffic flow and density is used to define the NFD. Conceptually, flow and density respectively represent the network production (trip completion rate) and accumulation (number of vehicles on the network). These variables are calculated as space-mean weighted averages of the link flows and densities (25), with link weights equal to the product of link length and number of lanes.

$$Q = \frac{\sum_{i=1}^M n_i l_i q_i}{\sum_{i=1}^M n_i l_i} \quad (1)$$

$$K = \frac{\sum_{i=1}^M n_i l_i k_i}{\sum_{i=1}^M n_i l_i} \quad (2)$$

where  $q$  and  $k$  are the link flow and density,  $Q$  and  $K$  are the weighted average flow and density values respectively,  $M$  is the number of links in the network,  $n$  is the number of lanes in each link, and  $l$  is the link length. This calculation in the context of this framework yields ordered pairs of macroscopic flow and density at 5 min time intervals which cumulatively form the simulation horizon. These values are plotted to give the NFD.

### Traffic Flow Simulation

Traffic simulation under the prevalent network and traffic conditions is a common step to model calibration and usage, as well as in the calculation of NFD and microscopic emissions. Dynamic traffic assignment (DTA) is a more suitable choice for this framework because it effectively incorporates the effects of traffic dynamics on the vehicular mechanical characteristics. DTA involves iteratively finding network user equilibrium based on the best paths in the network that keep changing because of variations in congestion with time while maintaining that no user can unilaterally decrease their travel time by changing the assigned route. This study uses the commercial traffic simulation tool PTV-Vissim for microscopic traffic simulations and DYNASMART-P for mesoscopic ones.

DTA-based traffic simulation results in detailed vehicular trajectories that include the vehicular properties, such as vehicle class and engine specifications, as well as dynamic properties such as position in the network, speed, and acceleration at each time step. The default simulation time steps of one and six seconds respectively in PTV-Vissim and DYNASMART-P are used for the simulation and generation of vehicle trajectories. Note that the six-second step size potentially masks the significant speed variations that can occur in this time. Moreover, mesoscopic simulation does not differentiate the values of speed and acceleration of individual vehicles moving on a given link at a given time step. These drawbacks of mesoscopic modeling are generally acceptable in the case of large networks since they are the only viable approach because of the size of the network. Furthermore, these important qualifications of mesoscopic simulators may be rendered insignificant if the resultant emission estimates can be calibrated against and proven similar to the more robust microscopic emission estimates. Thus, in this study both microscopic and mesoscopic simulation tools are utilized to model emissions for one medium and one large sized network.

In this study, it is assumed that the relevant traffic state of the network at any given time is represented by the NFD. In this regard, different sets of conditions, here

called ‘traffic scenarios’, are considered for training the emission estimation model in order to ensure its ability to work over a diverse range of common traffic states. Each traffic scenario leads to an observed network-wide flow-density relation (observed NFD) and is characterized by several factors that are known to influence the shape and existence of the NFD. These factors include network size and configuration, traffic demand and capacity, traffic composition, signal timing, dynamic user behavior, and incidents as well as local weather conditions (33). Two key variable factors used as inputs to the traffic simulator are demand level and profile, and prevalence of adaptive drivers, which are shown to have significant impacts on network traffic state (34–36).

### Traffic Composition

Vehicular emission rates are significantly dependent on the size of vehicle and its engine and fuel characteristics. Based on factors such as the microscopic emission model used, a simplified nested traffic composition scheme with four vehicle types is considered for a two-level modeling process based on size and fuel type. In this classification scheme, vehicles are first categorized as either light (cars, vans, and sports utility vehicles) or heavy vehicles (buses, trucks, and tractor-trailers). The light vehicles are then classified on the basis of fuel type: petrol (gasoline), diesel, and liquefied petroleum gas (LPG). It is assumed that, for a given NFD, the proportion of heavy vehicles is fixed and therefore the fleet composition of the light vehicles can vary freely without affecting NFD. Thus, the variation of both size and fuel type can be effectively captured without significant increase of computational complexity. The choice of these specific subcategories is based on the availability of calibrated functional coefficients in the micro-emission model.

Since the internal composition of light vehicles is a direct and variable indicator of network-wide emissions, it is to be tested for a wide variety of combinations. For comprehensive and qualitative testing, uniform sampling is a good option. One way of generating these scenarios based on uniform sampling is with the use of the linear Diophantine equation  $p_{\text{petrol}} + p_{\text{diesel}} + p_{\text{LPG}} + p_{\text{heavy}} = 1$ , where  $p_i$  is the penetration rate of vehicle type  $i$ . Since the proportion of heavy vehicles is fixed and known, sets of the light vehicle composition variables,  $TC = (p_{\text{petrol}}, p_{\text{diesel}}, p_{\text{LPG}}, p_{\text{heavy}})$ , here called traffic composition sets, can be generated combinatorially at a specific uniform spacing using the number theory concept of the stars and bars problem (37). In this study, for  $p_{\text{heavy}} = 0.1$  and a spacing of 10%, that is,  $p_i \in \{0, 0.1, \dots, 0.9\}$ , a total of  $\binom{10+3-1}{3-1} = 55$  combinations are generated, labeled TC1 through TC55.

Once these sets are generated, the trajectories of the light vehicles can be assigned to a fuel type based on a weighted random number using the assumed proportions in each scenario.

### Micro-Emission Model

The methodology provided in this paper does not make any qualifications regarding the choice of a microscopic emission estimation model as long as it takes into account the dynamic behavior of traffic and the distinction between vehicle types. This study incorporates the polynomial model suggested by Panis et al. (13) given as:

$$E_n^p(t) = c_1^p + c_2^p v_n(t) + c_3^p v_n^2(t) + c_4^p a_n(t) + c_5^p a_n^2(t) + c_6^p v_n(t) a_n(t) \quad (3)$$

where  $E_n^p(t)$  denotes the emission rate of pollutant  $p$  (in grams/second) from a vehicle  $n$  at simulation interval  $t$ ,  $v(t)$  is the vehicle’s speed in that time interval (m/s),  $a(t)$  is its acceleration (m/s<sup>2</sup>), and  $c_1^p$  through  $c_6^p$  are coefficients of the fitted curve. For more details on the model calibration procedure and coefficients values, readers are referred to Panis et al. (13). The estimated values of micro-emission at different simulation intervals are aggregated for each 5 min time interval and values of macro-emission are calculated by summing the values of micro-emission over the simulation period.

Two air pollutants are considered in this study: carbon dioxide (CO<sub>2</sub>) and nitrogen oxides (NO<sub>x</sub>). These pollutants have significant environmental and health impacts and have been considered by various studies in the literature (2, 13, 38). NO<sub>x</sub> (which is mostly hydrocarbons derived from fossil fuels) is included in emission standards by many environmental agencies, such as Hong Kong’s Environmental Protection Department (1). CO<sub>2</sub> acts as a greenhouse gas which is a major cause of global warming, and the transportation sector is one of the largest contributors of CO<sub>2</sub> emissions worldwide (39, 40). Note that the methodology proposed here provides flexibility to incorporate other pollutants and vehicle types, as long as they fit the general structure of the micro-emission model used.

### Modeling Framework

This study uses a framework that systematically integrates a microscopic emission estimation model with a dynamic traffic assignment simulator to assess the emission characteristics of vehicles at network level. This model considers the vehicle dynamics at a macroscopic level by generating vehicle trajectories using both microscopic and mesoscopic simulation tools. This is a variation of the more general format of integration of cross-

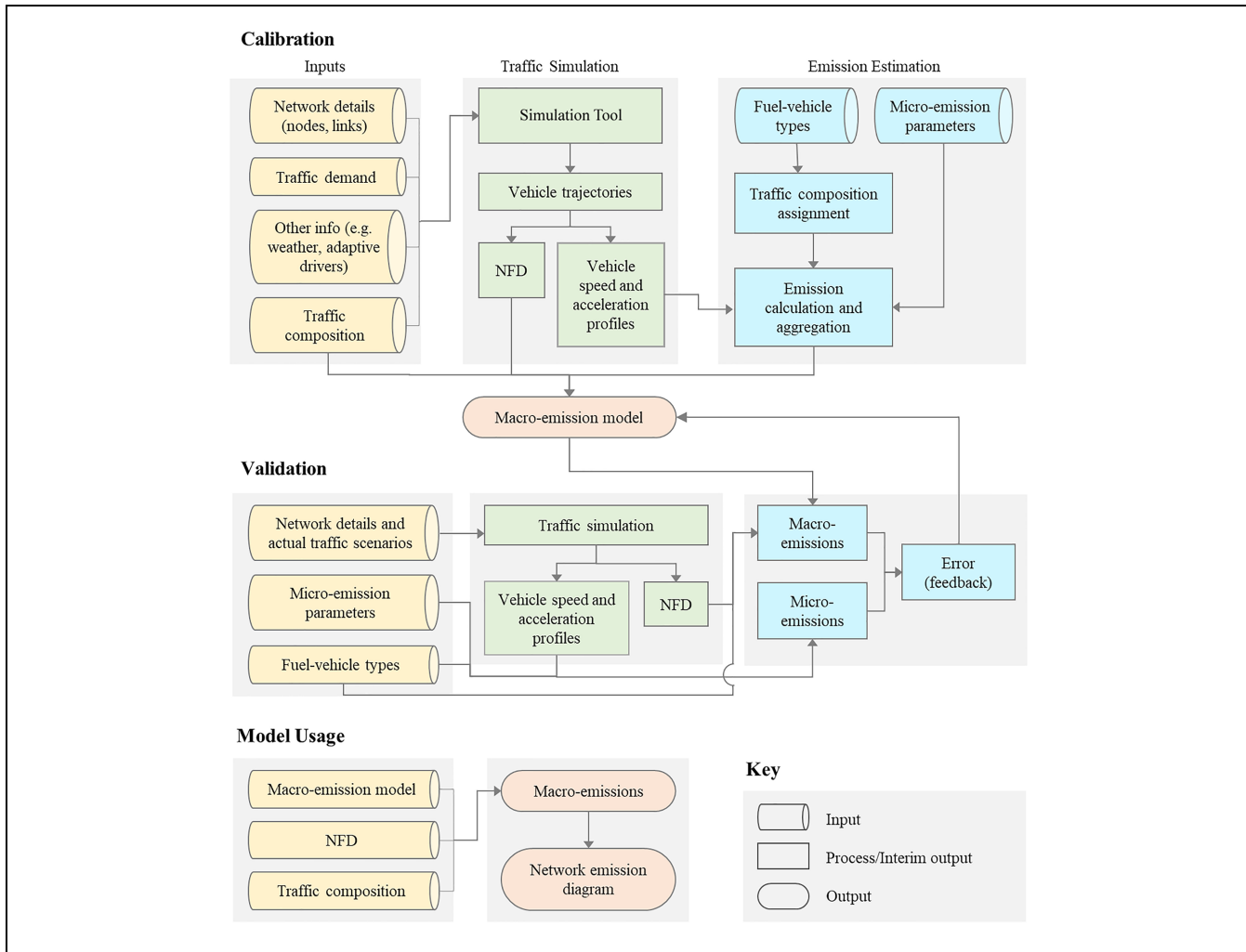


**Figure 1.** Research framework to estimate a macro-emission model.

Note: NFD = network fundamental diagram.

resolution modeling techniques, whose reliability has been sufficiently validated in the literature (22, 41).

The procedure followed in this study is illustrated in Figure 1. The schematic shows the respective steps to be followed for the creation of the model and its validation and application. The modeling process includes feeding network and traffic state inputs into the traffic simulator. The choice of this traffic simulation model largely depends on the size of the network. This study uses two traffic simulation techniques—microscopic and mesoscopic—to distinguish the applicability of these two types of techniques at two scales. Traffic simulation is used to generate two key outputs: aggregate traffic flow indicators and a set of vehicle trajectories. These data are then analyzed to generate NFD and network-wide emission estimates, which can be combined to visualize a network emission diagram (NED).

Two members of supervised learning models, non-linear regression and support vector machine

(SVM), are utilized to estimate the network-wide emissions by incorporating NFD and market penetration rates of different vehicle types in the network. SVM is mainly employed in classification contexts (42). It is also a well-recognized regression technique (43). Support vector regression (SVR) extends sophisticated binary classification via kernel trick to regression. In this study, an SVR model is generated with the input set  $\{K(t), Q(t), p_{\text{petrol}}, p_{\text{diesel}}, p_{\text{LPG}}, p_{\text{heavy}}\}$  and the radial basis function kernel as

$$\phi(u, v) = \exp(-\gamma \|u - v\|^2) \quad (4)$$

where the kernel function  $\phi$  measures the degree of similarity between feature vectors (rows of the dataset)  $u$  and  $v$ , and parameter  $\gamma$ , the number of independent variables, is chosen to be six. In addition to SVR, the following non-linear regression (NLR) model is also formulated as the macro-emission estimator.

$$\begin{aligned}
E_m^{(t)} &= \left( \sum_{i=1}^N \alpha_i^m p_i \right) K(t) (\beta_m + V(t)) \\
&= \left( \sum_{i=1}^N \alpha_i^m p_i \right) (\beta_m K(t) + Q(t))
\end{aligned} \tag{5}$$

where  $E_m$  is the rate of emission (in grams/second) of pollutant  $m \in \{\text{CO}_2, \text{NO}_x\}$  at time step  $t$  in the observation period,  $p_i$  is the penetration rate of vehicle type  $i$  in the traffic stream (1: petrol (gasoline) car, 2: diesel car, 3: LPG car, 4: heavy vehicle),  $K(t)$ ,  $V(t)$ , and  $Q(t)$  are respectively network-wide average density, speed, and flow, and  $\alpha_i^m$  and  $\beta_m$  are the model parameters for pollutant  $m$ .  $\beta_m$  represents the offset effect of average density, that is, the effect of density on emissions at very low speeds. A large value of this parameter implies high emission levels in the highly congested regime (in the limit case, it dictates the effect of traffic jam on emissions).

The proposed macro-emission model integrates the network-wide average density, as a representative of vehicle accumulation in the network, and average speed as the main incorporating factor in vehicular emission. The macro-emission model follows the structure of the underlying micro-emission model where the speed and its variation are the core factors. Multiplication of the network-wide average density aggregates the individual vehicles' emissions at network level. The aggregated value is then adjusted by a linear function of the penetration rates of vehicles powered by different fuels. More details will be presented in the next section.

## Numerical Experiment

Here, the proposed estimation framework is applied to a large-scale network and a medium-sized network to estimate the emissions. First, the study area and traffic scenario specifications are discussed, followed by the model calibration. To calibrate the model, actual data from 10 different days are utilized to generate traffic scenarios. The model is then validated by employing the actual data from the other three days. To comprehend better the relationship between network dynamics and emissions, a visualized form of the calibrated model for different pollutants is introduced, namely the NED.

### Study Area and Traffic Scenarios

The proposition of this study requires traffic information for a large urban road network. The city network of Chicago, Illinois, is selected as the study area. This network is a part of the Greater Chicago metropolitan area, one of the largest metropolitan areas in the United States. This network is bounded by O'Hare Airport to the west and Lake Michigan to the east. The schematic

of the network and its size parameters are shown in Figure 2a. To include the effects of network loading and unloading during peak and off-peak times, a simulation period of 5:00 a.m. to noon. is chosen in this study, which includes the morning peak time, as well as the off-peak periods before and after it. For the purpose of calibration of macroscopic emission modeling against the more effective microscopic modeling, a smaller region of this network is also analyzed. The central business district (CBD) region of this urban network (shown in the right part of Figure 2a) is simulated using a microscopic traffic simulator.

The network data was provided by the Chicago Metropolitan Agency for Planning. This data includes the network configuration and a base demand matrix. The demand profile of the base calibration scenario and the resultant NFD for both study networks are shown in Figure 2, *b* and *c*. The daily demand of the base scenario is 742,181 vehicles with a composition of 7% heavy and 93% light vehicles. For simplicity and clarity of creating traffic composition sets, a base case of 10% trucks is assumed for NFD generation and emission estimation.

The real-world data observed over 86 weekdays was used to create 86 variations of the base model. These observations include weather conditions, number of incidents, and total flow observed by 122 loop detectors. To limit the numerical experiments, 13 days with clear weather conditions were randomly selected for analysis and simulation, and an NFD was observed for each day. The selected scenarios were chosen from days with normal weather conditions to avoid considering the impact of weather condition on emissions. Ten of these NFDs were utilized to calibrate the proposed model (labeled C1–C10), while the remaining three were used for validation (V1–V3). The two parameters used to define these traffic scenarios were: aggregate daily traffic demand within the network, and the daily average percentage of adaptive drivers in the circulating traffic.

According to Figure 2c, the larger, low-density NFD of the city network contrasts sharply with the highly congested, smaller CBD network. The NFD progresses with time in a clockwise direction, with a steady increase in both flow and density during the loading phase up to the point of maximum flow and receding to the congested phase after that, with an increase in network density despite a drop in the throughput. In the recovery phase (the 2 h period of zero total demand), the network readily becomes empty, leading to a decrease in both flow and density, but the NFD does not follow the same path as of the loading period, resulting in hysteresis. NFDs of other scenarios are also observed to be shaped similarly and to exhibit hysteresis during the recovery phase. The variation of these NFDs is partly represented in Figure 3 using three network-level measures: maximum of the

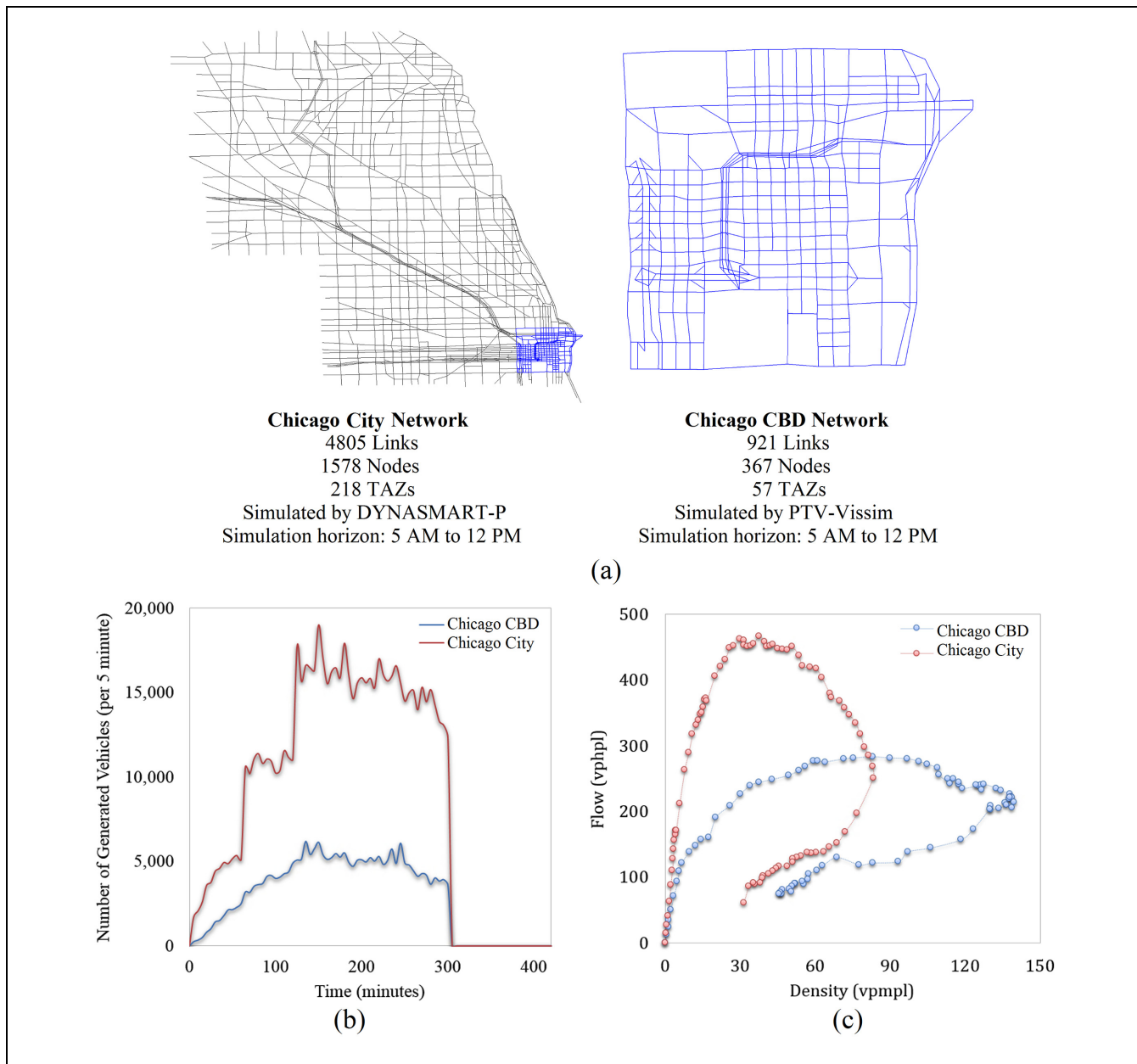


**Figure 2.** (a) Specifications of the study area, (b) simulated demand profiles, and (c) network fundamental diagrams of the Chicago city road network and its central business district. (Diagrams are for the base calibration scenario C5.)

Note: vphpl = vehicles per hour per lane; vpmpl = vehicles per mile per lane; CBD = central business district.

flow, maximum density, and the area of hysteresis loop. Since the results are the average values reported at network level, significant fluctuations are observed among different scenarios.

### Model Calibration

Generated emission values are calculated based on trajectory data and the macro-emission model for each pollutant and scenario at every 5 min time interval for the entire

simulation period by summing the values of emission rates (grams/second for micro-simulation or per six seconds for mesoscopic-simulation) over 5 min across all the links. It is observed that the macro-emission rate increases roughly parabolically with increasing density in the loading phase (see Figure 4, *a* and *c*). This is because of the fact that emission rates are more heavily dependent on individual vehicles' operational characteristics than their behavior as a group. It should also be noted that, despite the positive correlation of speed with emission rate in the microscopic



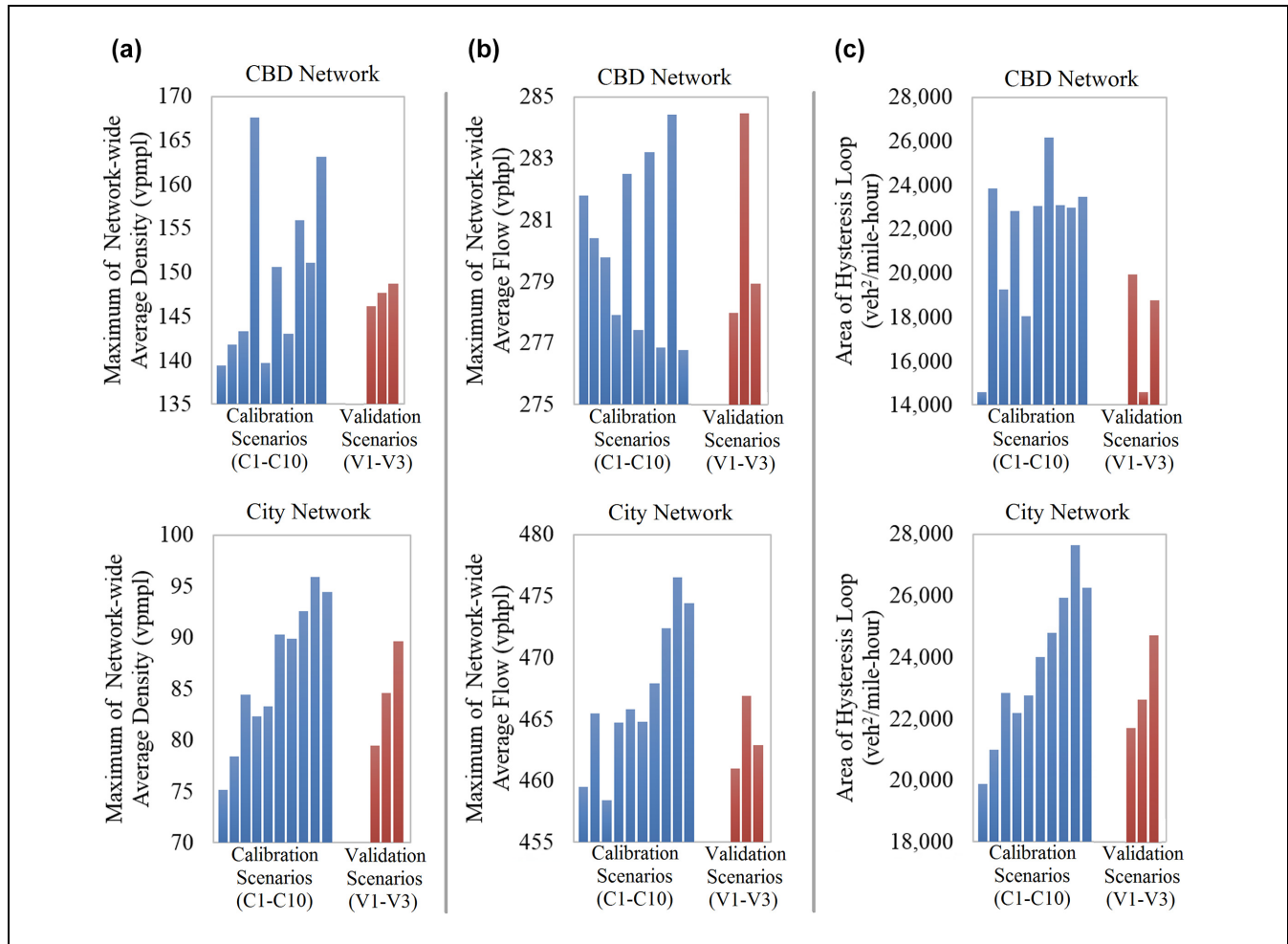


**Figure 3.** Variation of traffic flow characteristics across the different traffic scenarios: (a) maximum average flow, (b) maximum average density, and (c) area of hysteresis loop in NFD.

Note: vpmpl = vehicles per mile per lane; vphpl = vehicles per hour per lane; NFD = network fundamental diagram; CBD = central business district.

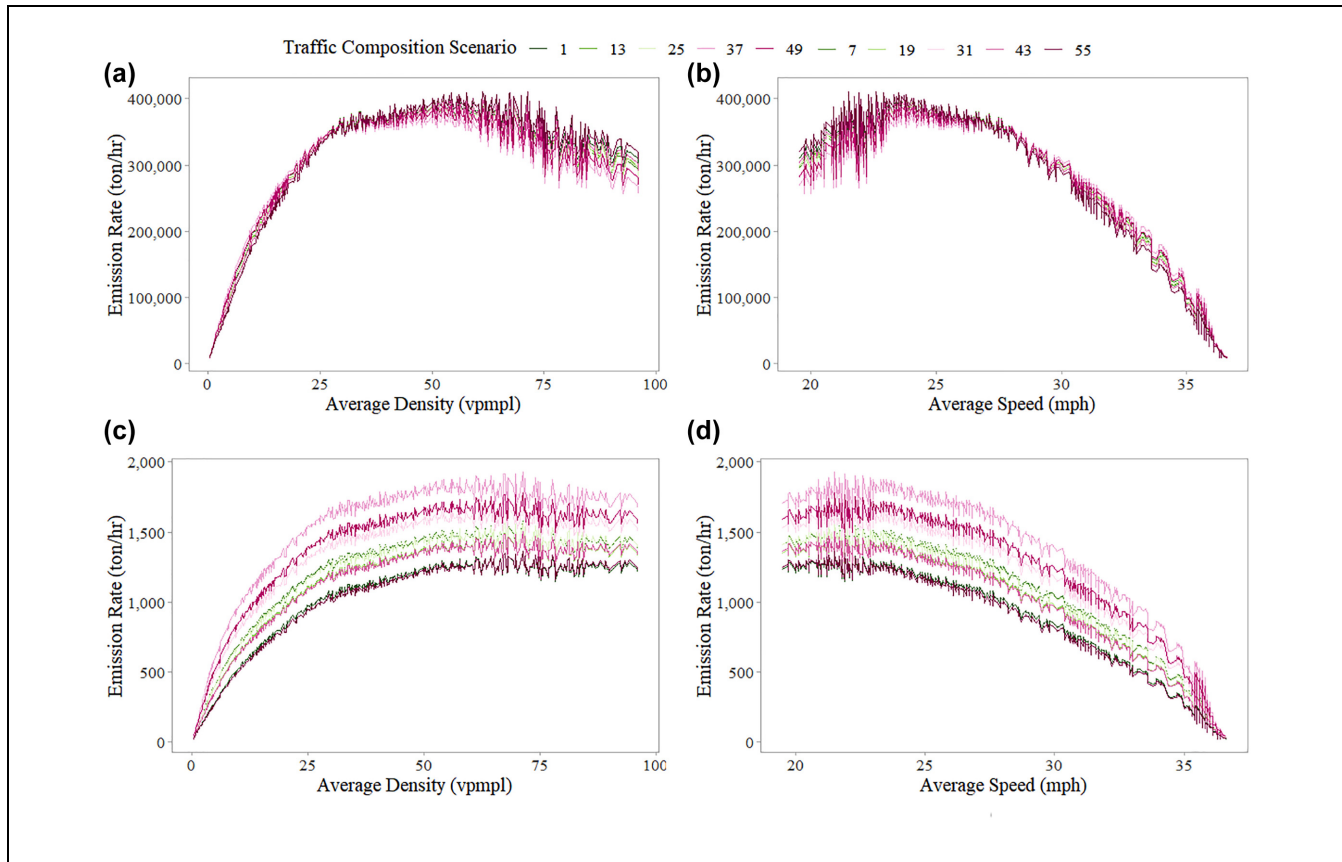
model, its effect is overshadowed by the effect of the network flow rate (throughput). This is evident in Figure 4, *b* and *d*, where the macro-emission rate increases at the network loading phase because of increased network average flow rate, in spite of a steady decrease in the average speed. Beyond the flow breakdown point, however, the emission generation rate decreases because of a reduction in both the average speed and the throughput in the network, although this pattern is less prominent in the case of  $\text{NO}_x$  (Figure 4*d*). In spite of reduced emission rates in the congested phase, the longer clearance time for the congested traffic because of reduced flow rates implies higher overall pollution in this phase.

Figure 4 also signifies the independent effect of traffic composition of light vehicles on emission. For demonstration, 10 traffic composition sets are uniformly and exhaustively selected and analyzed as seen by the different colored curves in Figure 4. They show that for the

same value of speed and density, different traffic composition sets only have a scaling effect. Therefore, the model can be simplified by considering a linear combination of the different proportions in the composition set as an independent predictor variable (see Equation 5).

The values of the calibrated coefficients of Equation 6 for the given study areas are presented in Table 1. The *p*-values associated with all the variables are either exactly or extremely close to zero, and the R-squared values are very close to one, indicating a strong curve fit. Note that the estimated parameters are completely different in two networks, which shows that these parameters need to be calibrated for each network and cannot be transferred. Thus, every application requires a calibration process based on detailed analysis of simulation results or available data sets. Using the 10 traffic scenarios, an SVR model is also trained to estimate the network-wide emission. Traffic state at every 5 min interval and the market





**Figure 4.** Scaling effect of vehicle type percentages on macro emission model in the loading phase of NFD—CBD network, micro-simulation: (a) emission versus density for  $\text{CO}_2$ , (b) emission versus speed for  $\text{CO}_2$ , (c) emission versus density for  $\text{NO}_x$ , and (d) emission versus speed for  $\text{NO}_x$  for 10 traffic composition scenarios in the calibration scenario *C1*.

Note: vpmp = vehicles per mile per lane; NFD = network fundamental diagram; CBD = central business district.

**Table 1.** Parameters of the Proposed Macro-Emission Model for the Pollutants Considered

Network	Pollutant	$\alpha_1$	$\alpha_2$	$\alpha_3$	$\alpha_4$	$\beta$	Adjusted $R^2$
CBD (microscopic)	$\text{CO}_2$	57.52	47.48	59.14	273.6	2.604	0.98
	$\text{NO}_x$	0.088	0.172	0.089	0.580	6.629	0.99
City (mesoscopic)	$\text{CO}_2$	483.6	450.6	484.9	2365	2.305	0.99
	$\text{NO}_x$	1.139	2.210	1.125	7.458	4.686	0.98

Note: CBD = central business district.

penetration rates of different vehicle types are provided to tune the SVR model. The average calibration runtimes of the NLR and SVR models for different pollutants and networks are 0.035 and 3.917 seconds, respectively. These results are obtained using a computer with i7-6700 octa-core CPU with a 3.4GHz clock and 16GB memory. It can be seen that SVR training is much more computationally consuming than NLR. In the next sections, it is shown that it also performs slightly better than NLR, leading to the common speed-accuracy tradeoff.

### Model Validation

The calibrated models are validated using the three validation scenarios. The NFDs of the base and validation scenarios are significantly different in relation to congestion pattern (see Figure 3). The effectiveness of the validation is quantified using the average of mean absolute relative error (MARE) of the model across each validation scenario. MARE is a widely used error metric that uses range normalization. For a pollutant  $m$ , it is given as:

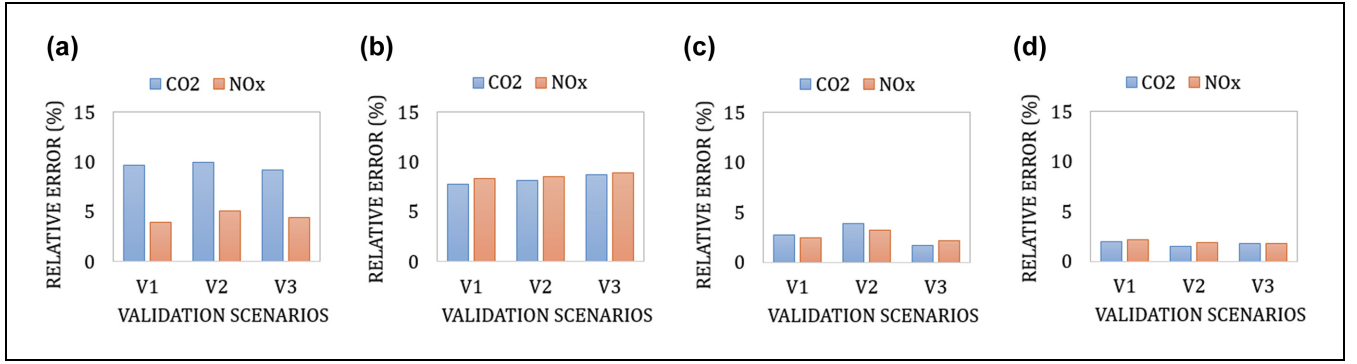


**Figure 5.** Mean absolute relative error in macroscopic emission estimation using the (a) non-linear regression model for CBD, (b) non-linear regression model for city network, (c) support vector regression model for CBD, and (d) support vector regression model for city network.

Note: CBD = central business district.

$$\epsilon_m = \frac{1}{N_C \cdot N_t} \left( \sum_{c=1}^{N_C} \sum_{t=1}^{N_t} \left| \frac{\hat{E}_{c,t}^m - E_{c,t}^m}{E_{c,t}^m} \right| \right) \times 100 \quad (6)$$

where  $E_{c,t}^m$  and  $\hat{E}_{c,t}^m$  are the estimates of emission rate of pollutant  $m$  at simulation time step  $t$  for traffic composition set  $c$  made by the reference microscopic emission model and the calibrated macroscopic model.  $N_C$  is the number of traffic composition sets (in this case, 55), and  $N_t$  is the number of time steps in the simulation period (84 5-min time intervals for a period of 7 h). The values of MARE obtained for the validation scenarios are shown in Figure 5. It can be seen that all values are reasonably low at the aggregate level, lying below 10%. The figures show that the SVR model performs better than the NLR model in all validation scenarios, with an error rate in the range of 2–5%. Based on very low error values in the validation scheme, the proposed NLR and SVR models (Equation 6 and Table 1) are considered valid for application at the study area. Examination of the error distributions across different traffic states did not show any particular pattern, leading to the conclusion that the errors over different traffic phases are random. Based on this conclusion and very low error values in the validation scheme, the proposed NLR and SVR models (Equation 6 and Table 1) are considered valid for application at the study area. In summary, the SVR method outperforms NLR, but it must be noted that SVR requires significantly more computation than NLR, and unlike NLR does not provide a closed-form expression for emission rate. The choice of model, either NLR or SVR, thus depends on the practitioner's preferences. Furthermore, there is no meaningful difference in performance of SVR or NLR for the CBD and city networks that were simulated by microscopic and mesoscopic simulation tools, respectively.

The proposed macro-emission model has some approximations relative to the micro-emission model

that is used for its calibration and validation. Unlike the micro-emission model, however, once it is calibrated, it does not require detailed trajectories of all traveling vehicles. It only incorporates the network-wide average flow and density given by an available NFD, and the traffic composition, which can be estimated for any given network with various approaches (e.g., see 28, 29, 44). This makes the proposed model a perfect tool for real-time control of emissions, unlike the micro model. Furthermore, it can be used for planning purposes simply by changing the traffic composition for the desired scenarios.

The qualitative nature of the inferences made by this model is presented in the next section. Note that in addition to estimating the exact emission rate, the model can capture the variations of the emission rate over the simulation horizon. This is based on a new concept, which is defined as the network emission diagram.

## Network Emission Diagram

The network emission diagram (NED) is here defined as a graphical representation of the relative network-wide emission rates and traffic state variations represented by the network-wide average values of flow and density. It is a three-dimensional graph whose projection on the density-flow plane is simply the NFD. In this case, different NEDs are obtained for different pollutants across different traffic scenarios and traffic compositions. Figure 6 illustrates an example NED for CO<sub>2</sub> in the traffic scenario V2 and traffic composition set TC25, in which the percentage of each category of light vehicles is 30% and heavy vehicles comprise the other 10%. This figure depicts the three-dimensional NED of CO<sub>2</sub> and its projections on the two traffic flow variable planes. This figure shows that the model successfully captures variations of the emission generation rate over the simulation horizon with an acceptable precision.

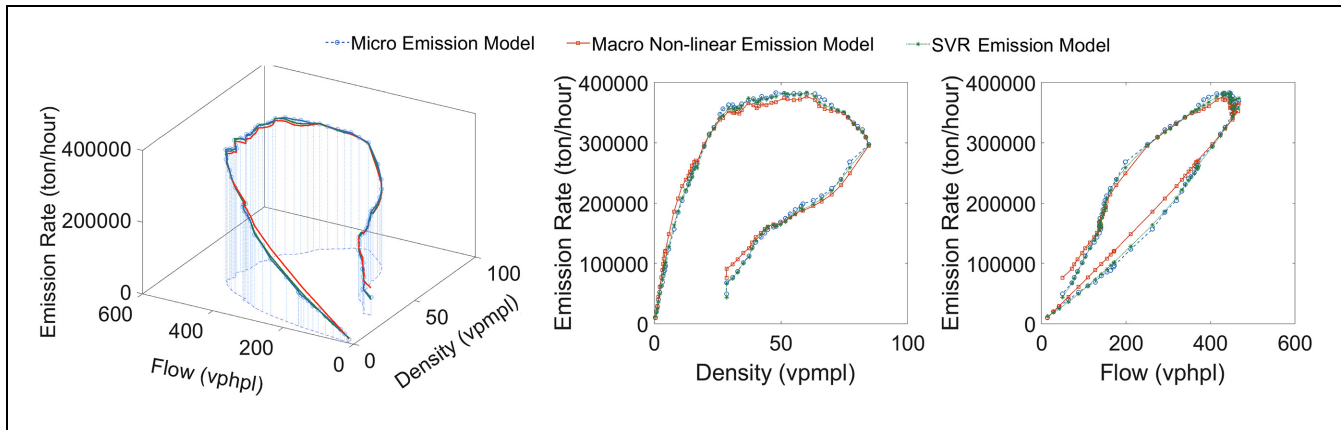


**Figure 6.** Network emission diagram of CO<sub>2</sub> for the city network for traffic composition set TC25 in the base validation scenario V2 for the macro non-linear and support vector regression (SVR) emission models, and the base micro-emission model.

Note: vphpl = vehicles per hour per lane; vpmp = vehicles per mile per lane.

Some important properties of NED can be inferred from Figure 6 that are key factors in the analysis of environmental impacts of the network loading mechanism. Macro-emission reaches its peak value at the peak traffic flow. This follows from the highly correlated variations of emission with the traffic flow, which is highly intuitive. This variation is not strictly linear, however, and the slopes are different in the two phases. The observations of NEDs of all pollutants show that the flow breakpoint segregates the flow-emission diagram into two phases: stable and unstable. For the same flow in the network, the unstable phase has higher emission rates compared with the stable phase. The unloading phase, characterized by recovering traffic with high density and low speed, is also considered a part of the unstable phase in this case. It can be hypothesized that this occurs because of higher density in the unstable phase, which may have a higher impact than the effect of lower speed in the unstable phase.

Figure 6 illustrates that the emission rate increases rapidly with increase in density and reaches a saturation level of maximum at high densities during the loading phase. Then, the flow breakdown occurs and emission rate decreases by density increase until the recovery (unloading phase) begins. The emission rate drops significantly during the unloading phase, reaching its minimum before reloading begins. This is a complementary observation to the varying slopes of the emission function with respect to flow. As mentioned earlier, the unstable phase (loading phase after flow breakdown) experiences higher emission rates compared with the stable phase (loading phase before the flow breakdown).

Flow breakdown results in emission rate reduction and it is because of the slowed down vehicles trapped in the gridlock. During the unstable phase (after the flow

breakdown), which is stretched out until the unloading begins, the network-wide average speed and throughput continually decrease and result in lower emission rates. It should be noted that it takes a longer time for a more congested network to recover from the gridlock. During the unstable phase, vehicles spend more time in the network and produce more emissions. Therefore, although the emission rate is decreased for the unstable phase, vehicles stay in the network for longer times and generate more emissions. So, more congestion results in more cumulative emissions overall. Figure 7 illustrates the NFDs, emission rates, and cumulative emissions for the city network for two distinct scenarios. This figure demonstrates that a more congested network produces more emissions overall despite the different pattern observed in its NED diagram. Note that the more congested scenario would recover much later than the less congested one, increasing the overall generated emissions.

Furthermore, the phenomenon of a clockwise and counter-clockwise hysteresis loop can be observed in the emission rate-density and emission rate-flow diagrams, respectively. The existence of the hysteresis loop states that the emission rate is multi-valued for both flow and density. For the same amount of flow, there is a higher emission rate in the unstable phase, owing to the dominant effect of higher density compared with that of lower speed. Also, the maximum emission rate is experienced when the network average flow is near its maximum. A similar phenomenon of multivaluedness is also observed in the emission-density graph. Unlike the emission-flow diagram, however, it starts at the beginning of the unloading phase and the emission rate is higher during the loading phase.

Another relevant conclusion that can be drawn from the comparison of NEDs across all scenarios is that the

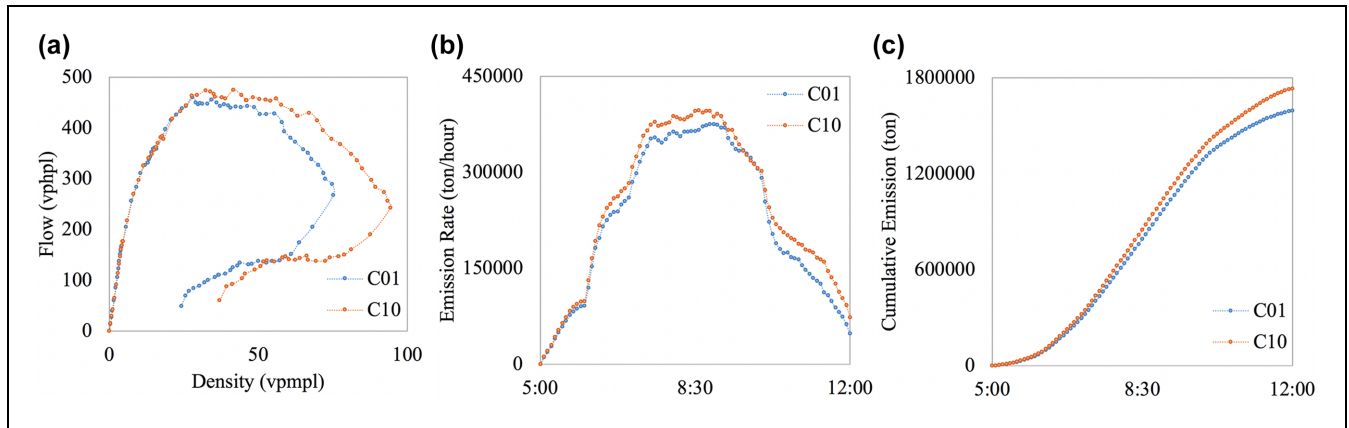


**Figure 7.** (a) Network fundamental diagram, (b) emission rates, and (c) cumulative emissions for two scenarios of C01 and C10 for the city network.

Note: vphpl = vehicles per hour per lane; vpmpl = vehicles per mile per lane.

rates of emission vary with the distribution of light vehicles in the network. For example, the increase in the percentage of diesel cars consistently results in an increase in the emission of  $\text{NO}_x$ . A similar case is observed for  $\text{CO}_2$  with variations in the percentage of diesel and LPG cars, providing further credibility to the model proposed in this study. These observations collectively provide reasonable evidence for the existence of NED as a general concept. In future studies, the importance and interpretation of this concept will be investigated in detail.

## Conclusion

This paper focuses on utilizing the concept of NFD in conjunction with a microscopic emission estimation model to derive an analytical model of emissions at the urban network level. It involves using network-level traffic demand data to simulate multiple network fundamental diagrams, that is, sets of macroscopic aggregate flow, density, and speed, and using these diagrams as base feed for a micro-emission model. A macro-emission model is then developed by simulation of different traffic demand and composition scenarios. Once the macro-emission model is calibrated and validated in a specific network, it can be deployed in daily operations for emission estimation addressing typical variations in demand and vehicle composition.

This technique is useful in theory because of its fast operation and requirement for minimal data of the type that is usually readily accessible from transportation planning and management agencies. It can be used for real-time traffic management for monitoring network-wide vehicular emissions. One such possible use case is measuring the impact of trucks and other heavy vehicles on air pollution in the dense business districts of large cities and forming the statistical basis for the suggestion

of policies like perimeter gating and congestion pricing. The detailed implementation of such applications is subject to future studies. The proposed framework is laid out in a general manner, which, with suitable modifications, allows for transferability to development of other macro-emission models. This generality also facilitates the extension of this framework to other cases, like the inclusion of other conventional and alternative fuel vehicles for a more rigorous analysis of these fuel types on a macroscopic level.

This framework is applied in this study on the Chicago city network as well as its dense CBD area. It is demonstrated that while microscopic traffic simulation yields better estimates of macro-emission, it can be replaced with the more resource efficient mesoscopic simulation on larger networks such as the city network, where micro simulation is not feasible because of computational complexity, without a substantial loss of accuracy. Therefore, this study recommends adopting a proper traffic simulator depending on the network size to estimate the macro-emission models to be used for real-time emission monitoring applications. Moreover, a proper regression model needs to be selected depending on the available computational resources. The numerical experiments in this study showed that although SVR outperforms NLR, both models provide acceptable approximations in the validation scenarios.

The results of the proposed model strongly support the existence of a relationship between emissions and the traffic state of the network represented by its NFD. The data currently available from the Chicago network is typical of that for many metropolises. The proposed model can also be improved with the addition of a large and diverse dataset covering a wide array of possible traffic states.

This paper also explores the relationship between macro-emissions and NFD with the help of an

introductory concept called the network emission diagram (NED), a three-dimensional curve showing the relationship between aggregate emissions and network average flow and density. Based on the NED, the maximum emission rate occurs at about the maximum network average flow right before the network breakdown because of congestion. The results of NED analysis suggest that the multivaluedness of emission rates for emission-flow and emission-density diagrams occur at the breakdown and unloading point, respectively. It is important to note that while this study postulates the existence of NED based on simulation results, it is essential to test these analyses on real-world observations. Also, the observations made in this study can be affected by the existence of variable emission rates, specifically for electric vehicles with zero tailpipe emissions, as well as under different weather conditions, which constitutes a reasonable future research direction. Furthermore, the conceptualization and observation of some of the properties of the NED provide direction for significant future work in the area of analysis of transportation networks regarding environmental concerns.

### Author Contributions

All the authors: Ramin Saedi, Rajat Verma, Ali Zockaie, Mehrnaz Ghamami, and Timothy J. Gates, contributed to all aspects of the study from conception and design, to data collection, to analysis and interpretation of results, and manuscript preparation. All authors reviewed the results and approved the final version of the manuscript.

### Declaration of Conflicting Interests

The author(s) declared no potential conflicts of interest with respect to the research, authorship, and/or publication of this article.

### Funding

The author(s) received no financial support for the research, authorship, and/or publication of this article.

### References

1. Cen, X., H. K. Lo, and L. Li. A Framework for Estimating Traffic Emissions: The Development of Passenger Car Emission Unit. *Transportation Research Part D: Transport and Environment*, Vol. 44, 2016, pp. 78–92. <https://doi.org/10.1016/j.trd.2016.02.013>.
2. Jiang, Y. Q., P. J. Ma, and S. G. Zhou. Macroscopic Modeling Approach to Estimate Traffic-Related Emissions in Urban Areas. *Transportation Research Part D: Transport and Environment*, Vol. 60, 2018, pp. 41–55. <https://doi.org/10.1016/j.trd.2015.10.022>.
3. Grote, M., I. Williams, J. Preston, and S. Kemp. Including Congestion Effects in Urban Road Traffic CO<sub>2</sub> Emissions Modelling: Do Local Government Authorities Have the Right Options? *Transportation Research Part D: Transport and Environment*, Vol. 43, 2016, pp. 95–106. <https://doi.org/10.1016/j.trd.2015.12.010>.
4. Kumar Pathak, S., V. Sood, Y. Singh, and S. A. Channiwala. Real World Vehicle Emissions: Their Correlation with Driving Parameters. *Transportation Research Part D: Transport and Environment*, Vol. 44, 2016, pp. 157–176. <https://doi.org/10.1016/j.trd.2016.02.001>.
5. Ahn, K., H. Rakha, A. Trani, and M. Van Aerde. Estimating Vehicle Fuel Consumption and Emissions Based on Instantaneous Speed and Acceleration Levels. *Journal of Transportation Engineering*, Vol. 128, No. 2, 2002, pp. 182–190.
6. Noland, R. B., W. Y. Ochieng, M. A. Quddus, R. J. North, and J. W. Polak. The Vehicle Emissions and Performance Monitoring System: Analysis of Tailpipe Emissions and Vehicle Performance. *Transportation Planning and Technology*, Vol. 27, No. 6, 2004, pp. 431–447. <https://doi.org/10.1080/0308106042000293480>.
7. Ntziachristos, L., and Z. Samaras. *COPERT II Computer Programme to Calculate Emissions from Road Transport*. Technical Report No. 49. European Environment Agency, Copenhagen, Denmark, 2000.
8. Boulter, P. G., T. Barlow, I. McCrae, S. Latham, D. Elst, and E. van de Burgwal. *Road Traffic Characteristics, Driving Patterns and Emission Factors for Congested Situations*. Report. Transportation Research Laboratory, Wokingham, UK, The Netherlands Organization for Applied Scientific Research, Delft, The Netherlands, 2002.
9. Han, K., H. Liu, V. V. Gayah, T. L. Friesz, and T. Yao. A Robust Optimization Approach for Dynamic Traffic Signal Control with Emission Considerations. *Transportation Research Part C: Emerging Technologies*, Vol. 70, 2016, pp. 3–26. <https://doi.org/10.1016/j.trc.2015.04.001>.
10. Qi, Y., H. Teng, and L. Yu. Microscale Emission Models Incorporating Acceleration and Deceleration. *Journal of Transportation Engineering*, Vol. 130, No. 3, 2004, pp. 348–359.
11. El-Shawarby, I., K. Ahn, and H. Rakha. Comparative Field Evaluation of Vehicle Cruise Speed and Acceleration Level Impacts on Hot Stabilized Emissions. *Transportation Research Part D: Transport and Environment*, Vol. 10, No. 1, 2005, pp. 13–30. <https://doi.org/https://doi.org/10.1016/j.trd.2004.09.002>.
12. Zegeye, S. K., B. De Schutter, J. Hellendoorn, E. A. Breunese, and A. Hegyi. Integrated Macroscopic Traffic Flow, Emission, and Fuel Consumption Model for Control Purposes. *Transportation Research Part C: Emerging Technologies*, Vol. 31, 2013, pp. 158–171. <https://doi.org/10.1016/j.trc.2013.01.002>.
13. Int Panis, L., S. Broekx, and R. Liu. Modelling Instantaneous Traffic Emission and the Influence of Traffic Speed Limits. *Science of the Total Environment*, Vol. 371, No. 1–3, 2006, pp. 270–285. <https://doi.org/10.1016/j.scitotenv.2006.08.017>.
14. Barceló, J. *Fundamentals of Traffic Simulation*. Springer, New York, 2010.
15. Sun, Z., P. Hao, X. (Jeff) Ban, and D. Yang. Trajectory-Based Vehicle Energy/Emissions Estimation for Signalized



- Arterials Using Mobile Sensing Data. *Transportation Research Part D: Transport and Environment*, Vol. 34, 2015, pp. 27–40. <https://doi.org/10.1016/j.trd.2014.10.005>.
16. Dia, H., S. Panwai, N. Boongrapue, T. Ton, and N. Smith. Comparative Evaluation of Power-Based Environmental Emissions Models. *Proc., 2006 IEEE Intelligent Transportation Systems Conference*, Toronto, Ontario, Canada, IEEE, New York, 2006, pp. 1251–1256.
  17. *User's Guide to MOBILE6.1 and MOBILE6.2: Mobile Source Emission Factor Model*. U.S. Environmental Protection Agency, Ann Arbor, MI, 2002.
  18. California Air Resources Board. *EMFAC 2007: Calculating Emission Inventories for Vehicles in California*. California Air Resources Board, Sacramento, CA, 2007.
  19. Ntziachristos, L., D. Gkatzoflias, C. Kouridis, and Z. Samaras. COPERT: A European Road Transport Emission Inventory Model. *Proc., 4th International ICSC Symposium Thessaloniki Information Technologies in Environmental Engineering* (I. N. Athanasiadis, A. E. Rizzoli, P. A. Mitkas, and J. M. Gómez, eds.). Springer, Berlin, 2009, pp. 491–504.
  20. Ahn, K. *Microscopic Fuel Consumption and Emission Modeling*. PhD dissertation. Virginia Polytechnic Institute and State University, Blacksburg, VA, 1999.
  21. Gori, S., S. La Spada, L. Mannini, and M. Nigro. A Dynamic Mesoscopic Emission Model for Signalized Intersections. *Proc., 16th International IEEE Conference on Intelligent Transportation Systems*, The Hague, Netherlands, IEEE, New York, 2013.
  22. Jamshidnejad, A., I. Papamichail, M. Papageorgiou, and B. De Schutter. A Mesoscopic Integrated Urban Traffic Flow-Emission Model. *Transportation Research Part C: Emerging Technologies*, Vol. 75, 2017, pp. 45–83. <https://doi.org/10.1016/j.trc.2016.11.024>.
  23. Shabihkhani, R., and E. J. Gonzales. Analytical Model for Vehicle Emissions at Signalized Intersection: Integrating Traffic and Microscopic Emissions Models. Presented at 92nd Annual Meeting of the Transportation Research Board, Washington, D.C., 2013.
  24. Alsalhi, R., V. V. Dixit, and V. V. Gayah. On the Existence of Network Macroscopic Safety Diagrams: Theory, Simulation and Empirical Evidence. *PLoS One*, Vol. 13, No. 8, 2018, p. e0200541.
  25. Geroliminis, N., and C. F. Daganzo. Existence of Urban-Scale Macroscopic Fundamental Diagrams: Some Experimental Findings. *Transportation Research Part B: Methodological*, Vol. 42, No. 9, 2008, pp. 759–770.
  26. Mahmassani, H. S., J. C. Williams, and R. Herman. Investigation of Network-Level Traffic Flow Relationships: Some Simulation Results. *Transportation Research Record: Journal of the Transportation Research Board*, 1984. 971: 121–130.
  27. Saberi, M., H. Mahmassani, T. Hou, and A. Zockaie. Estimating Network Fundamental Diagram Using Three-Dimensional Vehicle Trajectories. *Transportation Research Record: Journal of the Transportation Research Board*, 2014. 2422: 12–20.
  28. Zockaie, A., M. Saberi, and R. Saedi. A Resource Allocation Problem to Estimate Network Fundamental Diagram in Heterogeneous Networks: Optimal Locating of Fixed Measurement Points and Sampling of Probe Trajectories. *Transportation Research Part C: Emerging Technologies*, Vol. 86, 2018, pp. 245–262.
  29. Kaviani-pour, M., R. Saedi, A. Zockaie, and M. Saberi. Traffic State Estimation in Heterogeneous Networks with Stochastic Demand and Supply: Mixed Lagrangian-Eulerian Approach. *Transportation Research Record: Journal of the Transportation Research Board*, 2019. 2673: 114–126.
  30. Mahmassani, H. S., T. Hou, and M. Saberi. Connecting Networkwide Travel Time Reliability and the Network Fundamental Diagram of Traffic Flow. *Transportation Research Record: Journal of the Transportation Research Board*, 2013. 2391: 80–91.
  31. Castrillon, F., and J. Laval. Impact of Buses on the Macroscopic Fundamental Diagram of Homogeneous Arterial Corridors. *Transportmetrica B: Transport Dynamics*, Vol. 6, No. 4, 2017, pp. 286–301. <https://doi.org/10.1080/21680566.2017.1314203>.
  32. Saedi, R., M. Saeedmanesh, A. Zockaie, M. Saberi, N. Geroliminis, and H. S. Mahmassani. Estimating Network Travel Time Reliability with Network Partitioning. *Transportation Research Part C: Emerging Technologies*, Vol. 112, 2020, pp. 46–61.
  33. Nesamani, K. S., L. Chu, M. G. McNally, and R. Jayakrishnan. Estimation of Vehicular Emissions by Capturing Traffic Variations. *Atmospheric Environment*, Vol. 41, No. 14, 2007, pp. 2996–3008. <https://doi.org/10.1016/j.atmosenv.2006.12.027>.
  34. Mahmassani, H. S., M. Saberi, and A. Zockaie. Urban Network Gridlock: Theory, Characteristics, and Dynamics. *Transportation Research Part C: Emerging Technologies*, Vol. 36, 2013, pp. 480–497. <https://doi.org/10.1016/j.trc.2013.07.002>.
  35. Ji, Y., W. Daamen, S. Hoogendoorn, S. Hoogendoorn-Lanser, and X. Qian. Investigating the Shape of the Macroscopic Fundamental Diagram Using Simulation Data. *Transportation Research Record: Journal of the Transportation Research Board*, 2010. 2161: 40–48. <https://doi.org/10.3141/2161-05>.
  36. Saberi, M., H. S. Mahmassani, and A. Zockaie. Network Capacity, Traffic Instability, and Adaptive Driving: Findings from Simulated Urban Network Experiments. *EURO Journal on Transportation and Logistics*, Vol. 3, No. 3–4, 2014, pp. 289–308. <https://doi.org/10.1007/s13676-013-0040-2>.
  37. Feller, W. *An Introduction to Probability Theory and its Applications*. John Wiley & Sons, New Delhi, 2008.
  38. Niemeier, U., C. Granier, L. Kornbluh, S. Walters, and G. P. Brasseur. Global Impact of Road Traffic on Atmospheric Chemical Composition and on Ozone Climate Forcing. *Journal of Geophysical Research*, Vol. 111, No. D9, 2006, p. D09301. <https://doi.org/10.1029/2005JD006407>.
  39. Liu, C., Y. O. Susilo, and A. Karlström. Estimating Changes in Transport CO<sub>2</sub> Emissions Due to Changes in Weather and Climate in Sweden. *Transportation Research Part D: Transport and Environment*, Vol. 49, 2016, pp. 172–187. <https://doi.org/10.1016/j.trd.2016.09.004>.
  40. López-Martínez, J. M., F. Jiménez, F. J. Páez-Ayuso, M. N. Flores-Holgado, A. N. Arenas, B. Arenas-Ramirez, and

- F. Aparicio-Izquierdo. Modelling the Fuel Consumption and Pollutant Emissions of the Urban Bus Fleet of the City of Madrid. *Transportation Research Part D: Transport and Environment*, Vol. 52, 2017, pp. 112–127. <https://doi.org/10.1016/j.trd.2017.02.016>.
41. Zhou, X., S. Tanvir, H. Lei, J. Taylor, B. Liu, N. M. Rouphail, and H. C. Frey. Integrating a Simplified Emission Estimation Model and Mesoscopic Dynamic Traffic Simulator to Efficiently Evaluate Emission Impacts of Traffic Management Strategies. *Transportation Research Part D: Transport and Environment*, Vol. 37, 2015, pp. 123–136. <https://doi.org/10.1016/j.trd.2015.04.013>.
42. Suykens, J. A. K., and J. Vandewalle. Least Squares Support Vector Machine Classifiers. *Neural Processing Letters*, Vol. 9, No. 3, 1999, pp. 293–300.
43. Smola, A. J., and B. Schölkopf. A Tutorial on Support Vector Regression. *Statistics and Computing*, Vol. 14, No. 3, 2004, pp. 199–222.
44. Saeedmanesh, M., A. Kouvelas, and N. Geroliminis. A Real-Time State Estimation Approach for Multi-Region MFD Traffic Systems Based on Extended Kalman Filter. Presented at 98th Annual Meeting of the Transportation Research Board, Washington, D.C., 2019.